Journal of Environmental Chemical Engineering 13 (2025) 118991

Contents lists available at ScienceDirect

Journal of Environmental Chemical Engineering

journal homepage: www.elsevier.com/locate/jece

Breathing green: Sustainable approaches for the reuse of FFP2 facemasks

María Carracedo-Pérez [a], Cristina Prieto [b], María Blanco-Vales [a], Beatriz Magariños [c], Clara López-Iglesias [a,*], Carlos A. García-González [a,*]

[a] AerogelsLab, I+D Farma Group (GI-1645), Department of Pharmacology, Pharmacy and Pharmaceutical Technology, Faculty of Pharmacy, iMATUS and Health Research Institute of Santiago de Compostela (IDIS), Universidade de Santiago de Compostela, Santiago de Compostela E-15782, Spain
[b] Novel Materials and Nanotechnology Group, Institute of Agrochemistry and Food Technology (IATA), Spanish Council for Scientific Research (CSIC), Paterna, Spain
[c] Department of Microbiology and Parasitology, Aquatic One Health Research Center (iARCUS), Faculty of Biology, CIBUS, Universidade de Santiago de Compostela, Santiago de Compostela 15782, Spain

ARTICLE INFO

Keywords:
Mechanical filter
Electrostatic filter
Sterilization
Supercritical fluid technology
Green processing

ABSTRACT

Facemasks are essential components in healthcare environments, but their disposal represents a significant environmental concern. This study proposes an optimized sterilization treatment for the reprocessing of electrostatic filter (*EF*) and mechanical filter (*MF*) facemasks using supercritical carbon dioxide ($scCO_2$) and hydrogen peroxide, achieving a Sterility Assurance Level (SAL) of 10^{-6} in microbial load. The performance of the facemasks was evaluated after 1, 5, and 10 cycles and compared with those subjected to ethylene oxide and to γ-rays sterilization procedures, in terms of filtration efficiency, breathability, electrostatic charges of the filters, and of mechanical properties of the elastic bands. Structural and chemical changes were characterized using SEM and FTIR. The findings demonstrated that $scCO_2$ treatment induced electrostatic charges in the MF, improving their filtration efficiency. The supercritical treatment also preserved the chemical and structural integrity of both types of filters. Results underscore the effectiveness of the $scCO_2$ method as a viable and sustainable alternative to conventional sterilization methods.

1. Introduction

Medical masks are a crucial element of personal protective equipment (PPE) in the prevention and control of infectious respiratory diseases. They are the most effective solution for capturing fine particles, providing an effective barrier against aerosols and respiratory particles that may contain pathogenic agents [1–3]. Masks endowed with at least 95 % filtration efficiency for particles larger than 0.3 μm and intended for single use are classified as FFP2 in Europe, N95 in the United States, and K95 in China [4].

FFP2 facemasks consist of multiple filtering layers, typically four to five, providing effective respiratory protection without significant airflow restriction [1]. The outer layer acts as a pre-filter, capturing large particles and thereby extending the lifespan of the inner filters, which can be electrostatic or mechanical [1]. Electrostatic filters are composed of microfibrous layers that attract and capture fine particles through electrostatic interactions, thereby enhancing filtration efficiency (F_E) without restricting airflow. In contrast, mechanical filters employ densely woven fibers to physically trap particles based on their size and shape [2]. Mechanical filters offer sustained filtration, even in circumstances with fluctuating humidity or extended utilization, in which electrostatic filters are not suitable due to reductions in F_E [3]. The inner layer is intended to be more comfortable, so the main components are soft, non-irritating, and absorbent. The novel trends in inner layers designs include also inorganic nanomaterials and coatings which present antimicrobial properties for added safety [5,6].

The relevance of facemasks was exemplified during the COVID-19 pandemic as an essential strategy to mitigate the spread of the virus among the general population, to protect the frontline healthcare workers and, overall, to save lives [3]. However, the use of FFP2 facemasks during this period brought to light a social and environmental challenge due to their reduced lifetime (single use) and massive disposal. Only in 2024, global mask consumption was estimated in 129, 000 million units per month, taking up to 450 years to degrade [7]. Moreover, during 2020 and subsequent years of the COVID-19 crisis, it is estimated that *ca.* 1560 million facemasks ended up in the oceans, corresponding to between 468.9 and 624.0 tons of plastic [8,9]. These alarming values encourage further investigation into the reuse of FFP2

* Corresponding authors.
E-mail addresses: claralopez.iglesias@usc.es (C. López-Iglesias), carlos.garcia@usc.es (C.A. García-González).

https://doi.org/10.1016/j.jece.2025.118991
Received 20 May 2025; Received in revised form 19 August 2025; Accepted 27 August 2025
Available online 30 August 2025

facemasks.

A significant concern to be addressed for this potential reuse is the accumulation of biological load, both on the surface and internal structure of the used facemasks. Their reuse in the absence of an appropriate sterilization process can result in the reintroduction of pathogens into the respiratory system of the user, significantly increasing the risk of infection, and neglecting the purpose of the use of this PPE [10,11]. Consequently, there is a need for the development of a sterilization technique that effectively inactivates all microorganisms present on the material while preserving the integrity and efficacy of the facemask after multiple sterilization cycles [12]. For healthcare products labeled as STERILE, the requirements and guidance for selecting a Sterility Assurance Level (SAL) established a logarithmic reduction of 6 (SAL-6). This means that, after exposing the most resistant microorganism, i.e. dry bacterial endospores, to the inactivation process, the probability of survival of this microorganism is one in a million [13]. Therefore, achieving a sterility assurance level (SAL) of 10^{-6} implies that the probability of survival for weaker microorganisms, such as viruses, other bacteria, or their vegetative forms, would be even lower.

Numerous studies have explored the sterilization of medical devices by validated and regulated techniques, such as steam sterilization, ethylene oxide (EO) sterilization, or gamma irradiation (γ-rays) [14,15]. Steam sterilization is a widespread high-temperature method, with high efficacy in eliminating microorganisms through the denaturation of cellular proteins and degradation of lipids and nucleic acids, main components of the cellular structure [16,17]. Steam sterilization is ideal for metallic medical devices but deforms and degrades polymeric filters of facemasks, thereby reducing their filtration capacity [18,19]. The presence of water during the process also requires subsequent drying of the facemask to make it reusable, involving a second thermal treatment. On the other hand, EO is a reactive epoxide and the most common chemical additive used today to sterilize temperature and/or liquid water-sensible medical devices [20,21]. This colorless gas denaturalizes proteins and nucleic acids of microorganisms, inhibiting their metabolic activity [14]. Being effective at moderate temperatures (50–60 °C), EO sterilization process requires long treatments (from 2 to 96 h) and a final ventilation (aeration) period to eliminate toxic EO residues [20]. Previous studies on EO sterilization of surgical facemasks demonstrated that no structural changes occurred in the tested materials [22,23], but hazardous EO residues can remain in the inner structure causing potential health risks ranging from acute symptoms (cough, headache or convulsions), to severe chronic effects (spontaneous abortions, neurologic dysfunction, cancers, or even genetic material mutations) even at very low contents (ppm levels) [24–26]. γ-rays sterilization emerges as an alternative technique with no toxic residues, which is based on ionizing radiation that breaks the DNA bonds of microorganisms, preventing their replication and causing their death [27,28]. Also, γ-rays sterilization allows the treatment of compounds sensitive to temperature and humidity, while offering a high penetration capacity [29]. γ-rays are especially useful for products where the integrity of the material structure is not critical, such as syringes or catheters. However, in the case of facemask sterilization, γ-rays method has been proven not suitable as it caused yellowing of the material and compromised its physicochemical integrity, decreasing filtration efficiency [30,31].

The above-mentioned disadvantages of common sterilization techniques urged the exploration of alternative and innovative methods [32–35]. Among them, supercritical carbon dioxide ($scCO_2$)-based sterilization emerges as a novel, green, and sustainable alternative [32,33]. $ScCO_2$ exhibits intermediate properties between a liquid and a gas, offering a liquid-like, tunable density along with gas-like diffusion capacity and low viscosity [32]. Especially, this distinctive combination enables deeper penetration into complex-structured materials, including nanopores. These properties make $scCO_2$ technology highly attractive for industrial applications such as coffee decaffeination, textile dyeing, and essential oil extraction. CO_2 is a potent greenhouse gas whose emissions must be urgently minimized. The future perspectives aimed for this technology lie in harnessing the residual CO_2 from other industrial processes, transforming what was once a waste product into a valuable resource. This circular economy approach not only allows the valorization of CO_2 but also represents a significant step forward in reducing our environmental footprint. Furthermore, the operational conditions are suitable for thermosensitive materials with minimal degradation or alteration of their properties due to the mild critical point of CO_2 (73.74 bar and 31.0 °C) [36]. Over the last years, different medical devices have been subjected to $scCO_2$ treatment resulting in different levels of microbial inactivation [34,35,37–40]. $ScCO_2$ sterilization allows the use of additives, like hydrogen peroxide or peracetic acid, to enhance the inactivation effect and reach the sterility levels required for some biomedical applications [41,42].

The present research evaluates the potential of $scCO_2$ sterilization technology as a facemask sterilization alternative, assessing its efficacy in terms of microbial inactivation, preservation of material integrity, and reusability for numerous cycles. A $scCO_2$ sterilization process using H_2O_2 as chemical additive for FFP2 facemasks was herein optimized and microbiologically evaluated. The filtration capacity, breathing resistance, electrostatic charge, and structural integrity of the materials were assessed to better understand the performance and durability of the facemasks after up to 10 sterilization cycles. Two types of FFP2 facemasks with differing filtration mechanisms were tested: facemasks with electrostatic filters (*EF facemasks*), and facemasks with mechanical filtration (*MF facemasks*). Results were compared with those obtained under standard steam, EO and γ-rays sterilization methods that reach SAL-6, to identify the advantages and limitations of the supercritical sterilization method regarding the FFP2 facemasks properties and performances.

2. Materials and methods

2.1. Materials

Two types of FFP2 facemasks were evaluated: FFP2 Naturcare® NR facemasks, provided by Bimedica (Barcelona, Spain), equipped with a multi-layered electrostatic filter (*EF facemasks*), and FFP2 PAL 9091 RD self-filtering facemasks, provided by PROVEIL® (Paterna, Spain), equipped with a nanofibrous mechanical filter (*MF facemasks*). For all the procedures, FFP2 facemasks were individually packed in thermosealed sterilization pouches from Soplaril Hispania (Barcelona, Spain). These pouches are made of medical grade polyester, shutterless polypropylene and medical grade paper, which avoids microbial penetration while allowing the penetrability of the sterilant agent, following the standard UNE-EN ISO 11140–1:2015 [43].

For the sterilization with $scCO_2$, the materials used were CO_2 (99.8 % purity) supplied by Nippon Gases (Madrid, Spain) and hydrogen peroxide (H_2O_2) 30 % (v/v) from Sigma-Aldrich (Madrid, Spain). Sterility biological indicators were *Bacillus pumilus* (ATCC 27142) spore strips (10^6 spores/strip) and *Bacillus stearothermophilus* (ATCC 7953) spore strips (10^6 spores/strip), both purchased from Sigma-Aldrich (Madrid, Spain), and *Bacillus atrophaeus* (cell line 9372) spore strips (2.4 ×106 spores/strip) obtained from Crosstex International (Rush, NY, USA). Trypticase soy broth (TSB) and trypto-casein soy agar (TSA) media were purchased from BIOKAR Diagnosis (Pantin, France).

2.2. Sterilization treatments used with FFP2 facemasks

2.2.1. Sterilization with $scCO_2$

Sterilization assays with $scCO_2$ were carried out in a 2-liter autoclave (Eurotechnica GmbH, Bargteheide, Germany). Different amounts of H_2O_2, from 1000 to 1330 ppm (mg/L of CO_2) were tested to evaluate the sterilization efficacy. Dry spore strips of the different standardized bioindicators (BIs: *B. pumilus*, *B. atrophaeus* and *B. stearothermophilus*) were thermosealed in sterilization pouches and placed in the high-pressure vessel. Then, the vessel was pressurized to 140 bar in 30 min and

maintained at 39 °C with constant stirring during 3 h, as was reported in a previous work [44]. The first two hours were performed in the batch mode (without CO_2 flow), whereas the last hour was carried out in the continuous mode with a constant CO_2 pumping flow of 25 g/min. To reach atmospheric pressure, a depressurization step was performed at 3.5 g/min. After the treatment, spore strips were seeded in TSB medium and incubated for 7 days at 37 °C in the case of *B. pumilus* and *B. atrophaeus*, and at 55 °C in the case of *B. stearothermophilus*. Bacterial growth was determined not only daily by optical evaluation of the turbidity in the tubes, but also by seeding the liquid medium on TSA Petri dishes on the seventh day. The process was determined to be sterilizing when there was no turbidity in the TSB medium after seven days of incubation and no bacterial growth on the TSA plate after incubating the transferred liquid for 24 h.

Once the optimal H_2O_2 content was defined (1100 ppm), batches of fourteen FFP2 masks were subjected to the $scCO_2$ treatment explained before. The efficacy of each sterilization treatment was assessed using *B. pumilus* dry spore strips located at three levels of the autoclave (top, middle, bottom). FFP2 facemasks were subjected to 1 cycle (*$scCO_2$_1* samples), 5 cycles (*$scCO_2$_5* samples) and 10 cycles (*$scCO_2$_10* samples) to evaluate the effect of several cycles of $scCO_2$ sterilization treatments on the masks. To better simulate real-life contamination conditions, where viruses and bacteria are typically transported in liquid droplets or vapor, the procedure was also tested against *B. pumilus* spore suspension. This form is less resistant than dry endospores but still more resistant than most viruses and bacteria, making it a relevant intermediate model [45]. The suspension (100 µL of 1.5–1.9 × 10^6 spores) was inoculated onto square pieces (4 cm^2) of both types of facemasks, following the procedure described by Santos-Rosales et al. (2022) [46]. After being subjected to the sterilization procedure, the square pieces were seeded in TSB medium and incubated for seven days. To assess the sterilization result, the liquid was transferred to TSA medium and incubated at 37 °C for 24 h.

2.2.2. Sterilization treatment with EO

Chemical sterilization was performed by Esterilización S.L. (Montmeló, Spain) based on ISO 11135:2014 [20]. The treatment was carried out in a SUOD142483 sterilizer (Suphatec S.L., Bigues i Riells, Spain) in which facemasks contained in sterilization pouches were subjected to EO at 55 °C for 4 h and with a minimum relative humidity (RH) of 40 %. Due to the EO toxicity, sequential ventilating steps were performed after the sterilization period. This step was performed to clean partially toxic EO possibly remanent in the facemasks following a safer procedure. The initial stage of the ventilation process involved subjecting the samples to a vacuum process for 21 min. Thereafter, a purge with fresh N_2 was conducted for 8 min at 600 mbar. Subsequently, the samples were subjected to a second vacuum period of 12 min, followed by an 8-min air venting step at 600 mbar. Finally, the samples were ventilated with fresh air at 500 mbar for 34 min. Sterile samples were obtained 48 h after the last ventilation step at atmospheric pressure.

2.2.3. Sterilization treatment with γ-rays

The thermosealed samples were subjected to 30.6 kGy of γ-ray irradiation from a ^{60}Co source. The sterilization was performed in a first-category radioactive institution IR/B-02/69 (Aragogamma S.L., Les Franqueses del Vallès, Spain) following the ISO 11137-A2:2020 [27]. The process was carried out at room temperature during 7.53 h.

2.3. Facemasks characterization

2.3.1. Filtration efficacy and breathing resistance

The filtration efficacy (F_E) of the tested FFP2 facemasks was measured using a PMFT 1000 M filter media tester (Palas GmbH, Karlsruhe, Germany) in accordance with the standards described in EN 149:2001 + A1:2009 [47]. A paraffin oil aerosol with particle sizes ranging from 0.141 to 4 µm was used for the penetration test, with an aerosol exposure time of 3 min. F_E for each facemask was determined following Eq. (1).

$$F_E(\%) = \left(1 - \frac{Downstream\ Particle\ Concentration}{Upstream\ Particle\ Concentration}\right) \times 100 \quad (1)$$

The breathing resistance or breathability is related to the pressure drop on facemasks, which was measured following the abovementioned standard by passing compressed air through the facemask at 160 L/min, simulating extreme exhalation conditions. For both tests, the samples of treated FFP2 facemasks were cut into 100 cm^2 pieces and analyzed in triplicate at 25 °C and 50 % RH.

2.3.2. Electrostatic charge characterization

The electrostatic charge of the samples was evaluated using an IZH10 electrostatic meter (SMC Corporation, Tokyo, Japan). The samples were placed on paper, and the static voltage was measured at 1 cm from the sample. The maximum and minimum values of each sample were recorded. Two replicates were taken from individual components, i.e. outer and inner polypropylene spunbonded layers and inner filters of both types of facemasks.

The retention of charges on the polymeric material was evaluated measuring the electrostatic charge after subjecting the samples to an electrostatic charge induction treatment using a LE500 electrospinning machine from Fluidnatek (Bioinicia S.L., Paterna, Spain) at a voltage between 15 and 20 kV during 5 min with 20 cm distance between the positive electrode and the sample.

2.3.3. Mechanical tests

Tensile tests were conducted on the elastic bands of both sterilized and non-sterilized FFP2 facemasks using a TA.XT Plus Texture Analyzer (Stable Micro Systems, Ltd., Surrey, UK), equipped with a 30 kg load cell and operating at a crosshead speed of 5 mm/s. This procedure was performed in accordance with ASTM standards [48]. Cuts of 50 mm length of the elastic bands were fixed between the upper and lower clamps, with a distance of 25 mm between each clamp. Subsequently, the elastic bands were subjected to five loading cycles. In each cycle, the elastic bands were extended by 25 mm, equivalent to 100 % deformation for the 25 mm spacing. Each sample was tested in duplicate at room temperature. The Young's modulus (E) of each sample was calculated from the stress-strain plots, with engineering stress and strain duly adjusted, as well as the maximum strength resisted (F_{max}).

2.3.4. Filter morphology characterization

Morphological changes of the facemasks were evaluated by scanning electron microscopy (SEM) (Hitachi S-4800, Hitachi High Technologies Corp., Tokyo, Japan) using an electron beam acceleration of 10 kV. Two samples from each sterilization technique were previously sputter coated with gold/palladium before imaging.

2.3.5. FTIR spectroscopy characterization

Bruker Tensor 37 FT-IR spectrometer (Bruker, Ettlingen, Germany) coupled to the ATR Golden Gate sampling accessory (Specac Ltd., Orpington, UK) was used to obtain ATR-FTIR spectra of untreated and treated mask filters. All spectra were recorded between 4000 and 600 cm^{-1}, with a resolution of 4 cm^{-1} and averaged over 10 scans. OPUS 4.0 software (Bruker, Ettlingen, Germany) was used to analyze the spectra.

2.4. Statistical analysis

Results were expressed as mean ± standard deviation and statistically analyzed using GraphPad Prism v.8.0.2 software (GraphPad Software, San Diego, CA, USA). Statistical analyses of F_E and ΔP results were performed using one-way ANOVA test, with subsequent Tukey's multiple comparison test. E and F_{max} results were statistically analyzed using

two-way ANOVA using Tukey's multiple comparison test. This approach enabled the comparison of values obtained after the first load/unload cycle with those obtained after the fifth cycle, each cycle being evaluated independently. Furthermore, a two-way ANOVA, followed by Šídák multiple comparison test, was employed to ascertain whether there were statistically significant differences between the values recorded in the initial cycle and those in the fifth load/unload cycle for each type of sample. Statistical tests were performed, assuming 95 % of significance level and the Null Hypothesis was that there was no difference between the means of the sample groups being analyzed.

3. Results and discussion

3.1. Evaluation of $scCO_2$ sterilization treatment

The bactericidal properties of $scCO_2$ are not strong enough to attain a SAL-6 against the most resistant microorganism required for medical devices labeled as STERILE [32,49]. To achieve this level, peracetic acid-based compounds have been extensively utilized as additives due to their potent oxidative properties, synergizing the activity of $scCO_2$ [50,51]. Alternatively, H_2O_2 has been identified as a superior chemical additive due to its capacity to sterilize with $scCO_2$ at reduced temperatures and at lower concentrations to achieve the same level of sterility [41,52]. Moreover, the use of H_2O_2 is advantageous since it rapidly forms hydroxyl radicals that attack DNA, membrane lipids and other essential bacterial cell components [53,54].

The efficiency of the $scCO_2$ sterilization process was assessed by performing batches at varying concentrations of H_2O_2, i.e. 1330, 1200, 1100, and 1000 ppm, using *B. pumilus* as BI as it was previously reported as the most resistant microorganism to $scCO_2$ treatment [34,42]. *B. atrophaeus* and *B. stearothermophilus*, standardized BIs for other sterilization techniques (steam and radiation sterilizations, respectively) were also tested [34,46]. The maximum concentration of 1330 ppm was selected as it was the lowest amount of H_2O_2 reported for the sterilization of other medical devices under mild working conditions [46].

Fig. 1 illustrates that the optimal concentration of H_2O_2 for the sterilization treatment was 1100 ppm, since this was the minimum concentration where SAL-6 was achieved. Also, the related resistance of the different BIs used to assess the sterility against this sterilization technique was shown. In previous work, *B. atrophaeus* was demonstrated weaker against this inactivation technique than *B. pumilus* [34]. In this work, the microbial resistance to $scCO_2$ sterilization was set in the following order: *B. pumilus* as the most resistant microorganisms, followed by *B. atrophaeus* and *B. stearothermophilus*.

The lower amount of H_2O_2 (1100 ppm) herein needed for sterilization compared to previous works (3330 ppm [34] and 1200 ppm [53]) was attributed to the different exposure regime. Previously, only dynamic (with CO_2 flow) or static/batch (CO_2 atmosphere without flow) processes were studied. In this work, a two-hour batch regime was followed by a one-hour period with continuous flow of fresh CO_2. Microbial inactivation could be enhanced due to two phenomena. On one hand, the static regime in the presence of agitation enhances the homogenization of the additive in the vessel. On the other hand, the continuous flow of CO_2 was designed to renew at least two times the CO_2 environment, allowing the removal of any remaining additive in the equipment and from the treated material, avoiding the need for post-aeration [34,39]. Due to the low solubility of H_2O_2 in the $scCO_2$ fluid, exposure time has to be longer than expected [55]. Furthermore, although the efficacy of this sterilization must be assessed against dry *B. pumilus* spores, since it is the most resistant microorganism for this sterilization technique, the most common microorganisms present in used facemasks are weaker and usually present as a liquid suspension, i.e. as vegetative cells [56]. In this context, the continuous flow of fresh $scCO_2$ also contributes to the inactivation of vegetative bacteria, since their cell membrane lipids are soluble in the $scCO_2$ environment [32]. On the other hand, the test conducted with square pieces (4 cm^2) against a liquid suspension of *B. pumilus* bacterial endospores resulted in an absence of contamination in the TSB tubes and TSA plates, thus, in complete microbial inactivation. This absence of contamination can be explained by the fact that the samples were subjected to a $scCO_2$ treatment specifically designed for the inactivation of dry bacterial endospores, which are the most resistant microorganisms. Moreover, milder operating conditions have been reported in the literature for the inactivation of SARS-CoV-2, a weaker microorganism than the tested in this work. For instance, Ruiz et al. (2025) achieved viral disinfection at 95 bar and 35 °C for 5 min using a combination of a commercial additive (NovaKill™) and 50 ppm H_2O_2 [57] and Zulli et al. (2024) demonstrated SARS-CoV-2 inactivation under conditions of 80 bar and 45 °C for 5 min in the presence of 50 ppm H_2O_2 [58].

It was reported that cycles of depressurization/pressurization enhanced microbial inactivation through mechanical bursting of the cells [39]. However, due to the combined regime procedure used in this work, a single depressurization step of 3.5 g/min rate was enough to provide sterility against dry spore strips of *B. pumilus* without compromising the integrity of the material. Previous studies also proved that low depressurization rates (1.2 g/min) are not enough for achieving SAL of $\leq 10^{-6}$ [34]. Finally, previous studies sterilized facemasks using $scCO_2$ using strips of dry spores of *B. stearothermophilus* and *B. atrophaeus* [57] or spore suspensions [46], that is under exposure to weaker microorganisms towards this procedure as herein demonstrated.

3.2. Effect of sterilization treatments on facemask performance

3.2.1. Filtration and Breathing Resistance performance

Filtration efficacy (F_E) and pressure drop (ΔP) are the main parameters indicating the performance of the facemask filters and were herein evaluated for the two types of FFP2 facemasks according to current standard procedures (Fig. 2). As expected, both untreated masks met the required standard of $F_E \geq 94$ % for a FFP2 mask classification, as set out in EN 149:2001 + A1:2009 (Fig. 2A,B) [47]. *EF facemask* (Fig. 2A)

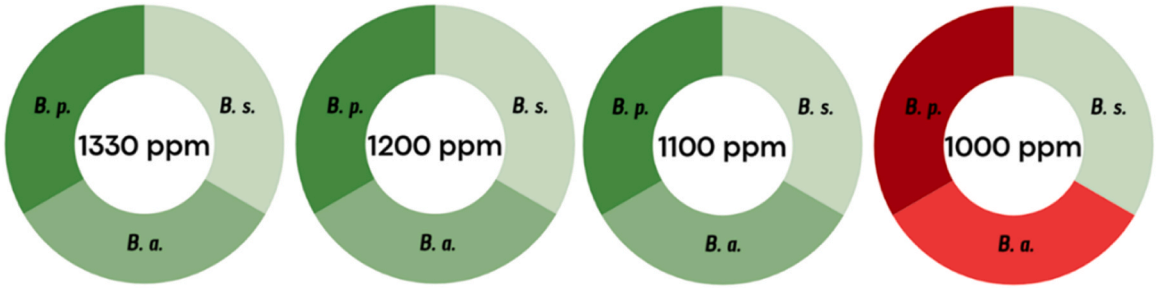

Fig. 1. Microbiological results obtained after the $scCO_2$ treatment tests with four varying H_2O_2 contents (from left to right): 1330, 1200, 1100 and 1000 ppm. Color intensity (dark/light) is correlated with microbial resistance to $scCO_2$ sterilization, with darker shades indicating higher resistance [34]. The green color represents SAL-6 achieved, while red indicates contamination, i.e. SAL-6 not achieved. Notation: B.s.: *Bacillus stearothermophilus*; B.a.: *Bacillus atrophaeus*; B.p.: *Bacillus pumilus*.

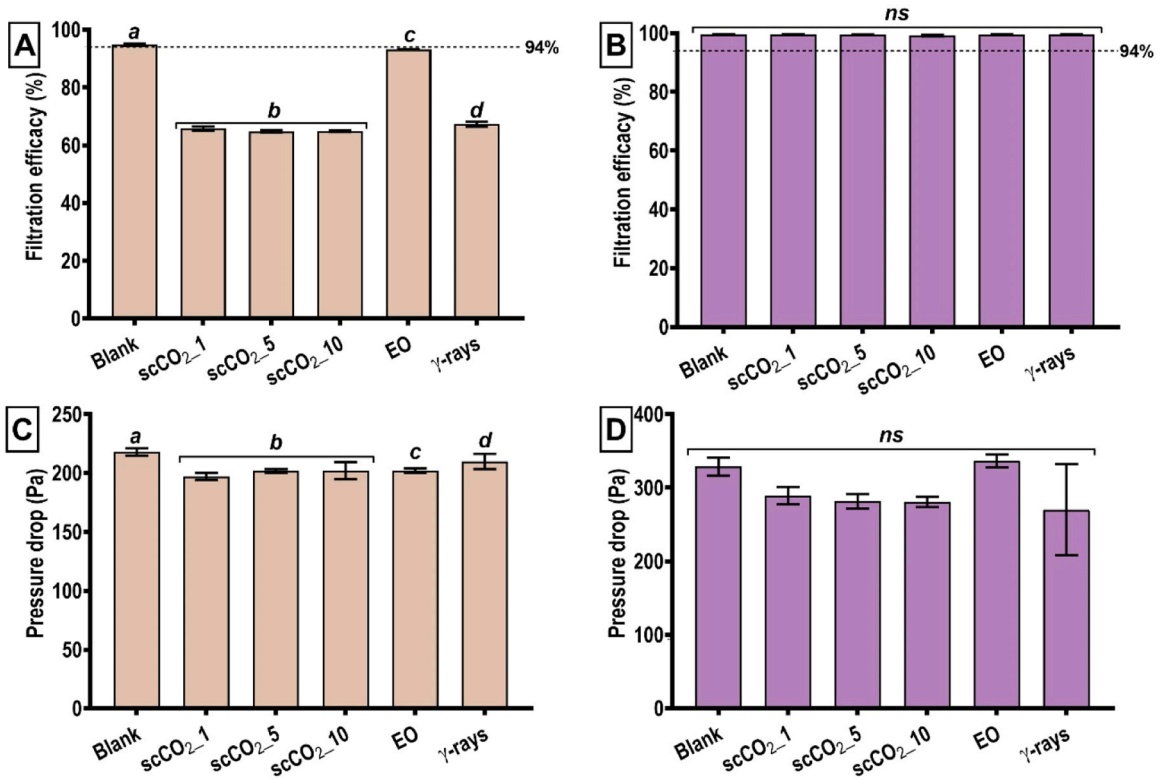

Fig. 2. Filtration efficacy (F_E) of (A) *EF* and (B) *MF FFP2 facemasks* and breathing resistance measured through the pressure drop (ΔP) of (C) *EF* and (D) *MF facemasks*. Equal letters denote statistically homogeneous groups. Horizontal dashed lines in (A) and (B) denote the minimum required F_E value following the standard EN 149:2001 + A1:2009 [47].

displayed a notable reduction in F_E, with a 30 % loss after 1 cycle of $scCO_2$ sterilization, without significant changes when increasing the cycles performed. EO treatment and γ-rays exposure caused a 2 % and a 30 % reduction in the F_E, respectively. In electrostatic filters, like the *EF facemask*, the observed changes in filtration efficacy could be caused by changes in the electrostatic charge and the structural integrity of the filter [59] so further tests were conducted in Section 3.2.2.

In contrast, *MF facemasks* (Fig. 2B) exhibited robust F_E following a range of treatments, demonstrating only an estimated 0.4 % decrease in efficiency after 10 treatments with $scCO_2$. These results suggest that *EF facemasks* are more sensitive to sterilization treatments than *MF facemasks*, being EO the mildest technique to modify the filtration efficiency.

Figs. 2C and 2D revealed the impact of the sterilization treatments regarding the ΔP as a qualitative measurement of respiratory resistance or breathability. In a tight or restrictive mask, the ΔP between the internal and external sides of the mask is high which means that breathing is more difficult. In contrast, masks that are highly transpirable result in a low value of ΔP [60]. With respect to *EF facemasks* (Fig. 2C), the reduction in ΔP after sterilization treatments shows a maximum of 10 %. The highest differences were observed in the facemasks treated with $scCO_2$ and EO compared to the untreated samples, while γ-rays treatment demonstrated less variation. No changes in ΔP of *EF facemasks* were observed from the first to the tenth $scCO_2$ cycle. The reduction in ΔP could be caused by the effect of the sterilization treatment on the mechanical properties of the filter [61], which was related to mechanical stress or degradation or oxidation reactions of the polymeric materials.

For the *MF facemask* case (Fig. 2D), ΔP exhibited lower values in the samples treated with $scCO_2$ than the untreated sample. Regarding EO treatment, no noteworthy discrepancies in ΔP were discerned with respect to the untreated facemask. In contrast, results obtained following γ-rays treatment showed a high degree of variability among the three samples analyzed. However, this variability is attributed to a material-specific behavior rather than to experimental errors during the analysis, and it does not compromise the robustness of the results or the conclusions regarding filtration performance. As documented in the literature, this type of radiation has the potential to impact the polymer chains, which may subsequently influence the mechanical properties of the materials [62,63], and consequently have an effect on pressure drop.

Both parameters (F_E and ΔP) may be combined into one in the so-called quality factor (Q) [64,65] using Eq. (2) as:

$$Q = -\ln(1- F_E)/\Delta P \quad (2)$$

A high Q value indicates a better performance of the mask, as a very efficient filter with low ΔP effectively retains particles while optimizing energy consumption or reducing respiratory effort. On the contrary, a low Q value implies a lower filtration efficiency, or a higher ΔP, which could result in higher respiratory effort or poorer filtration performance. To compare the different Q obtained for each sample, the relation between the Q of the sterilized samples ($Q_{Sterile}$) and the untreated ones (Q_{Blank}) was denoted as Q_F and calculated using Eq. (3):

$$Q_F(\%) = Q_{Sterile}/Q_{Blank} \times 100 \quad (3)$$

The Q_F obtained was represented in Figure S1 (Supplementary Data). In the case of *EF facemasks* Figure S1A, a decrease in Q_F can be appreciated after all sterilization treatments, especially when sterilized by γ-rays and $scCO_2$. In the latter, there was a slight decrease of Q_F when more cycles were applied. The values of Q_F in *MF facemasks* (Figure S1B) remained above those of the *Blank* even after the tenth cycle, although a reduction trend in Q_F was observed when multiple sterilization cycles with $scCO_2$ were carried out. This was due to a reduction in ΔP as the number of sterilization cycles increased, coupled with the observation that F_E was unaltered after exposure to $scCO_2$. Consequently, the use of $scCO_2$ as a sterilization technique may result in an enhancement of the overall quality of *MF facemasks*, but not in that of *EF facemasks*, since on them the decrease in F_E was quite notorious and did not meet the

standard.

3.2.2. Electrostatic filter performance

EF facemasks employ an electrostatic attraction mechanism to capture both charged and neutral particles in suspension. Accordingly, electrostatic tests were conducted to analyze the impact of sterilization treatments on the electrostatic charges of both types of facemasks. Moreover, the facemask filter samples were subjected to an electrostatic charge induction treatment to assess the retention of charges on the polymeric material. The filter layers of *EF facemasks* are composed of meltblown polypropylene (PP) and spunbond polyethylene (PE), and the filters of *MF facemasks* are composed of polyvinylidene fluoride (PVDF) nanofibers. The filters of *EF* and *MF facemasks* are outlined with green lines in Figs. 3A and 3B, respectively. Fig. 3C (*EF facemasks*) and 3D (*MF facemasks*) show density of positive (upper box) and negative (lower box) charges, and the median (intermediate horizontal line of the box) obtained before (light color) and after (dark color) the electrostatic charge induction on untreated and sterilized samples.

Blank sample (untreated) of *EF facemask* presented a high density of negative charges while the positives charges were nearly zero, with a net difference in electrostatic charges of 0.18 kV, in accordance with their filtration mechanism. The behavior of the filters in *EF facemasks* treated with $scCO_2$ had charge density distributed towards more negative charges, this effect being more noticeable as more sterilization cycles were performed. The electrostatic charge induction resulted in a significant increase in the difference between the positive and negative charges present in the filters in the *Blank* sample. Concurrently, the samples exposed to $scCO_2$ exhibited the same tendency observed before the charge induction, in an amplified way. Treatment with EO slightly increased the positive charges, but obtaining a similar net charge to *Blank* even after the induction treatment. In the case of exposure of the material to γ-rays, the charge distribution resulted in higher negative density values with a 0.28 kV difference between the average positive and average negative charges, i.e. 0.10 kV higher than the untreated sample (*Blank*).

On the other hand, the *Blank* sample of *MF facemasks* demonstrated a purely mechanical filtration mechanism since the net electrostatic charge presented a value approaching zero. In the filters treated with $scCO_2$, there was an increasing trend in the distribution density of electrostatic charges as the number of $scCO_2$ cycles increased. This means that this treatment caused a polarization of the charges, leading to an increase in both positive and negative values. Such effect was more evident after the charge induction treatment as also observed for the *EF facemasks*. Treatments involving EO and γ-rays did not alter this lack of electrostatic behavior of *MF facemasks*.

In both *EF facemasks* and *MF facemasks* filters, the sample *$scCO_2$_1* experienced similar tendencies in the electrostatic charge difference compared with *Blank* samples. After various cycles, the density of charges seemed to be more heterogeneously distributed, with *$scCO_2$_10* sample showing the highest difference between the positive and negative charge values in both cases. These experimental results obtained for $scCO_2$-treated samples suggest that this treatment induces new electrostatic charges. In the case of *EF facemasks*, these charges seemed to interact with the preexisting ones, thus modifying them. In *MF facemasks,* far from being a disadvantage, this effect may favor the capture of nanoparticles smaller than 100 nm, which mechanical filters often miss, through electrostatic forces. These changes in the electrostatic charges could explain why the filtration capacity of the *MF facemask* (observed

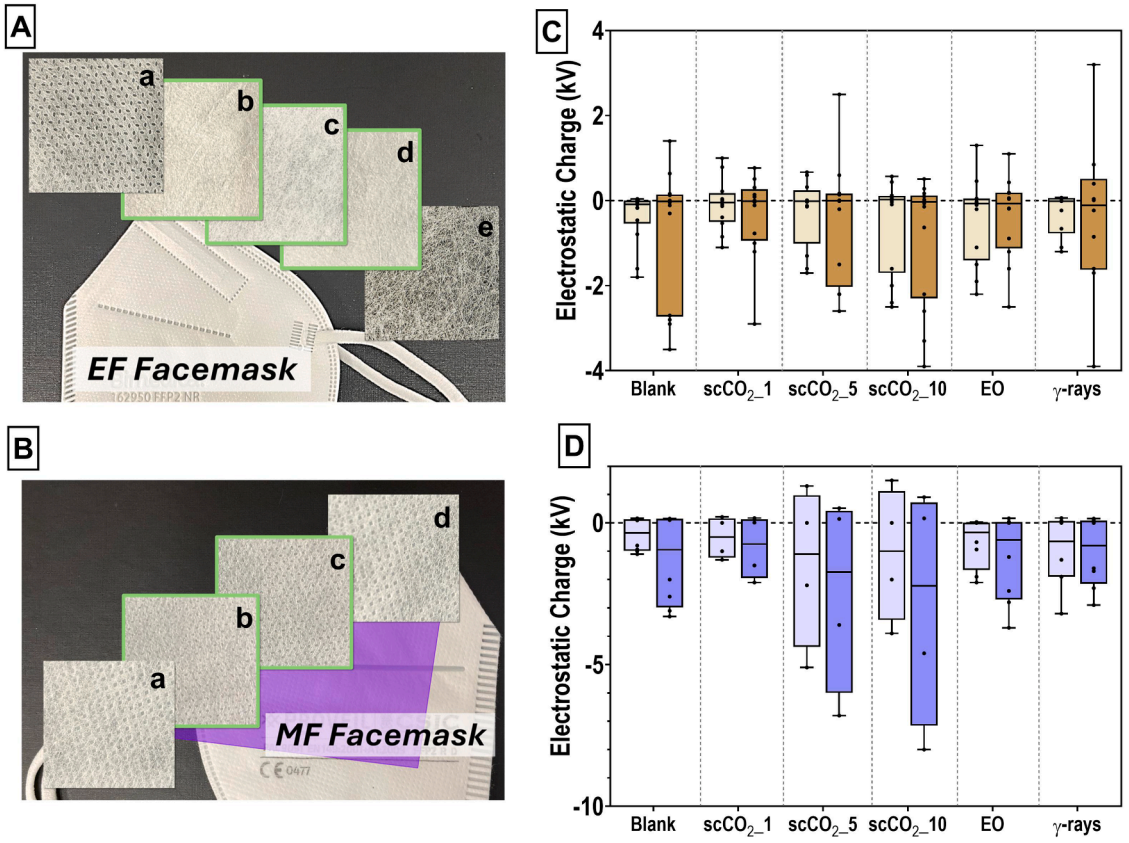

Fig. 3. Layers distribution of A) *EF facemask* (a) External spunbond PE filter, (b) meltblown PP and (c) spundbond PE, (d) meltblown PP filter and (e) internal PE spunbond filter; B) *MF facemask* (a) External spunbond PP filter, (b) and (c) spundbond PP plus electrospun nanofiber-based filter of PVDF (d) Internal PP spunbond filter. Distribution of the electrostatic charges for C) *EF facemask* and D) *MF facemask* filters. Light and dark color indicate values obtained before and after the electrostatic charge induction treatment, respectively. The bars correspond to the calculated electrostatic median value for each sample, with the exact values from each replicate represented with dots.

in Fig. 2B) remained above the required 94 %, while the *EF facemasks* did not meet the established requirement (Fig. 2A). Regarding the increase in electrostatic charges after $scCO_2$ treatment, the literature reported that the adsorption of $scCO_2$ onto polymeric fibers may induce surface charges [66]. Also, oxidation reactions caused by the H_2O_2 additive on the polymer surface may alter its chemical composition and increase the negative charges [67].

3.2.3. Mechanical performance of the elastic bands

The final stage of performance evaluation of the facemasks involved an analysis of the elastic bands to ascertain the impact of the different sterilization procedures on their elasticity and strength, which are key factors in maintaining effectiveness and user comfort. The elasticity was assessed based on the E modulus. F_{max} of the elastic bands represents the stress at which the elastic region ends and therefore, the deformation becomes permanent. All these results are collected in Table 1.

In the case of *MF facemasks,* both E and F_{max} values had similar tendencies and mainly dependent on the sterilization treatment. After the supercritical sterilization, a decrease in the E and F_{max} values was observed without significant differences with regards to the untreated sample and to the number of sterilization cycles, even after the fifth load/unload cycle. However, EO sterilization of *MF facemasks* noteworthy resulted in an increase on both the E and the F_{max} resisted by the elastic bands, and that this happened in the first and in the fifth loading cycles. For γ-rays sterilization, *MF facemask* bands remained without significant mechanical differences with respect to *Blank* sample.

3.3. Effect of sterilization treatments on physicochemical properties

3.3.1. Morphological changes

SEM images of *EF facemasks* and *MF facemasks* filters, both untreated and after the different sterilization treatments, are shown in Fig. 4. In the case of the PE filter in both untreated (Fig. 4.1a) and sterilized masks (Fig. 4.1b-f), cracks and significant porosity were visible immediately in the higher magnification images. In all cases, the cracks became more pronounced after the sterilization processes, which could be related to the slight decrease in the ΔP previously observed. The deepest cracks were observed after γ-rays and could be attributed to an increase of brittleness, due in turn to a radiation-induced oxidation of the material causing the breakage of covalent bonds [68]. The PP filter exhibited no noticeable changes before and after the sterilization treatments, as the fibers appeared tight and entangled in all cases (Fig. 4.2a-f). As shown in Figure S2, the PP filter fibers were analyzed at higher magnification, and no significant morphological changes were observed after the sterilization treatments. Although slight damage is visible in Figure S2c, it is likely related to pre-existing imperfections in the original facemasks rather than being a consequence of the $scCO_2$ sterilization process.

The morphology of the mechanical filter before and after the sterilization treatment that composes *MF facemasks* is presented in Fig. 4.3a-f. The untreated filter exhibited smooth and tense fibers and displayed a uniform morphology (Fig. 4.3a). Regarding the treatments involving CO_2, alterations in fiber morphology were observed, including fewer tense fibers and, in some cases, wavy fibers (Fig. 4.3b-d). This effect was more evident as more cycles of exposure to $scCO_2$ were applied to the samples, with *$scCO_2$_10* sample being the most affected, showing breakage of the thinner fibers. Similar alterations were appreciated in the case of EO treatment, since the breakage of thinner fibers was observed (Fig. 4.3e). However, the untreated sample characteristics remained consistent following treatment with γ-rays (Fig. 4.3 f). The fibers were observed at higher magnification (Figure S3). In the samples treated with $scCO_2$, a more pronounced fiber entanglement is evident due to the wavy appearance of the fibers. In contrast, the fibers treated with EO and γ-rays appear straighter and more tense, with the finer fibers being shorter and less entangled. The observed alterations in fiber morphology in response to $scCO_2$ sterilization can be attributed to three effects. First, manufacturing flaws of the nanofibers, which could also be seen in the other treatments, combined with the mechanical stress induced by the diffusion of CO_2 through the facemask, and the absorption of CO_2 within the fibers during the sterilization process. CO_2 can easily dissolve in fluorinated polymers such as PVDF in *MF facemasks*, causing them to swell [69]. For both types of fibers, a direct correlation between how wavy the fibers resulted after the $scCO_2$ sterilization treatment, and the ΔP values (Fig. 2C,D) could be considered. The increased fiber entanglement could enhance filtration efficacy, whereas the relaxation of the fibers might reduce filtration capacity. Especially in *MF facemasks*, the overall filtration performance of the facemasks may remain comparable, while offering improved breathability and comfort for the user.

3.3.2. Chemical changes by Infrared Spectroscopy

The chemical analysis was performed on both types of filters of the *EF facemasks*, i.e. spunbond PE (Fig. 5) and meltblown PP (Fig. 6), and on the PVDF filter of the *MF facemasks* (Fig. 7).

The main characteristic bands of PE polymer before and after the different sterilization treatments were found in the spunbond filter of *EF facemask* (Fig. 5). The bands at 2914 and 2848 cm^{-1} (enlarged in region 1 of Fig. 5) were related to the asymmetric and symmetric stretching, respectively, of the CH_2 group [70,71]. In the 600–1800 cm^{-1} range

Table 1
Young's modulus (E, kPa) and maximum strength (F_{max}, N) values for the facemask bands before (*Blank*) and after the different sterilization procedures for both types of facemasks (*EF* and *MF*). Results were statistically analyzed by first comparing the values after each load/unload cycle, where the same letter represents statistically homogeneous groups. Additionally, the first and fifth cycles of each sample were compared in pairs, where the symbol * indicates a significant difference between the pairs.

Sample	Treatment	E (kPa)		F_{max} (N)	
		1st cycle	5th cycle	1st cycle	5th cycle
EF facemasks	**Blank**	169.7 ± 11.2^{a}	170.2 ± 6.7^{c}	1.315 ± 0.005^{e}	1.262 ± 0.005^{g}
	$scCO_2$_1	153.5 ± 6.0^{a}	149.6 ± 3.1^{d}	1.214 ± 0.007^{f}	1.152 ± 0.010^{h}
	$scCO_2$_5	160.5 ± 1.1^{a}	$165.5 \pm 3.6^{c,d}$	$1.274 \pm 0.006^{e,f}$	$1.223 \pm 0.005^{g,h}$
	$scCO_2$_10	157.3 ± 1.3^{a}	$161.7 \pm 5.6^{c,d}$	$1.257 \pm 0.051^{e,f}$	$1.168 \pm 0.032^{h*}$
	EO	161.2 ± 4.3^{a}	$160.9 \pm 7.7^{c,d}$	$1.239 \pm 0.046^{e,f}$	$1.176 \pm 0.042^{g,h}$
	γ-rays	156.0 ± 4.2^{a}	$158.8 \pm 6.3^{c,d}$	$1.250 \pm 0.039^{e,f}$	1.166 ± 0.011^{h}
MF facemasks	**Blank**	$166.0 \pm 0.0^{a',b'}$	$170.5 \pm 0.4^{c',d'}$	$1.321 \pm 0.007^{e'}$	$1.264 \pm 0.007^{g',h'}$
	$scCO_2$_1	$158.4 \pm 3.7^{a'}$	$170.5 \pm 2.4^{c',d'*}$	$1.296 \pm 0.007^{e'}$	$1.222 \pm 0.017^{g'*}$
	$scCO_2$_5	$156.6 \pm 0.9^{a'}$	$171.3 \pm 2.6^{c',d'*}$	$1.295 \pm 0.030^{e'}$	$1.215 \pm 0.018^{g'*}$
	$scCO_2$_10	$158.7 \pm 5.8^{a'}$	$164.5 \pm 5.9^{c',d'}$	$1.290 \pm 0.046^{e'}$	$1.213 \pm 0.024^{g'*}$
	EO	$168.4 \pm 0.8^{b'}$	$173.9 \pm 0.0^{c'}$	$1.403 \pm 0.017^{f'}$	$1.315 \pm 0.005^{h'*}$
	γ-rays	$165.0 \pm 0.0^{a',b}$	$163.0 \pm 0.0^{d'}$	$1.322 \pm 0.028^{e'}$	$1.256 \pm 0.027^{g',h'}$

For *EF facemask*, E and F_{max} results showed a slight decrease on all sterilized facemasks bands with respect to *Blank* sample. The results did not present significant differences after the first load/unload cycle, except for the case of *$scCO_2$_1* sample. A trend of reduction in the values appeared after the fifth load/unload cycle, especially in the *$scCO_2$_1* sample.

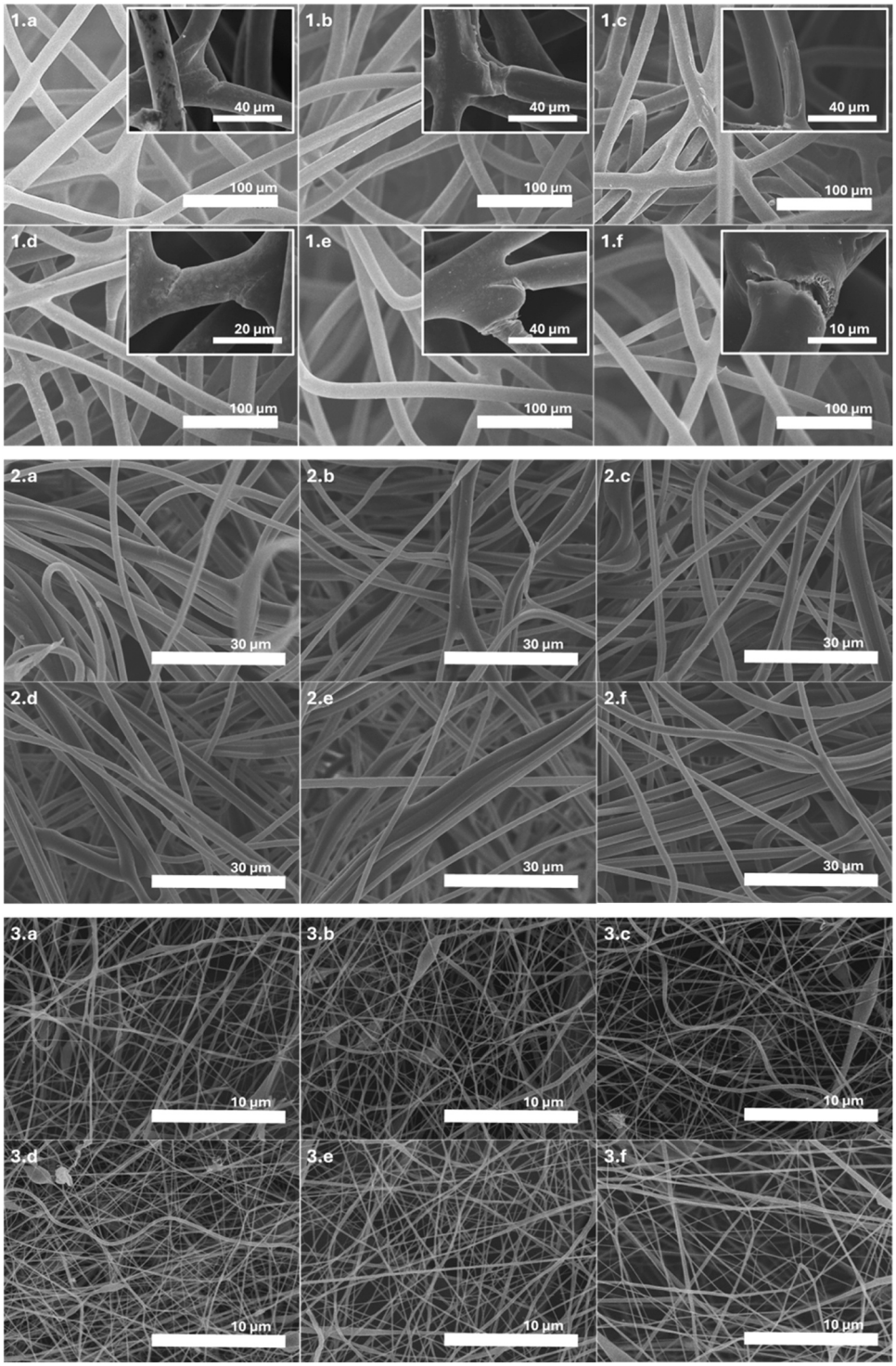

Fig. 4. SEM images of (1) PE and (2) PP filters of *EF facemasks*, (3) PVDF filter of *MF facemasks*. Sterilization treatment: (a) Untreated, (b) $scCO_2$_1, (c) $scCO_2$_5, (d) $scCO_2$_10, (e) EO and (f) γ-rays samples.

(region 2 in Fig. 5), the bands associated to CH_2 bending (1462 cm^{-1}) and CH_2 rocking (718 cm^{-1}) were found, thus completing the PE backbone. Moreover, two wide bands located at 1713 and 1239 cm^{-1} corresponded to the stretching of the C═O group. The PE spunbond filter of *$scCO_2$_1* and *$scCO_2$_5* facemask samples had similar spectra compared with the untreated sample, but *$scCO_2$_10*, *γ-rays* and *EO* samples presented higher intensities in the bands at 1239, 1713 and 2848 cm^{-1}. On one hand, γ-rays and EO could induce the oxidation of the polymer resulting in polar groups (C═O, -OH), disrupting CH_2 dipole symmetry and, thus, resulting in higher intensities and wider C═O stretching bands, like the ones located at 1713 cm^{-1} [72]. This effect could be slightly more appreciated after 10 cycles of $scCO_2$ sterilization (*$scCO_2$_10*) since this sample has been repeatedly subjected to CO_2 in the presence of H_2O_2, which is a strong oxidant used for enhancing the sterilization treatment efficacy, and could lead to the degradation of PE [72,73].

Fig. 6 shows the FTIR spectra of the meltblown PP filters of the *EF facemask*. In the region between 2800 and 3000 cm^{-1} (region 1 in

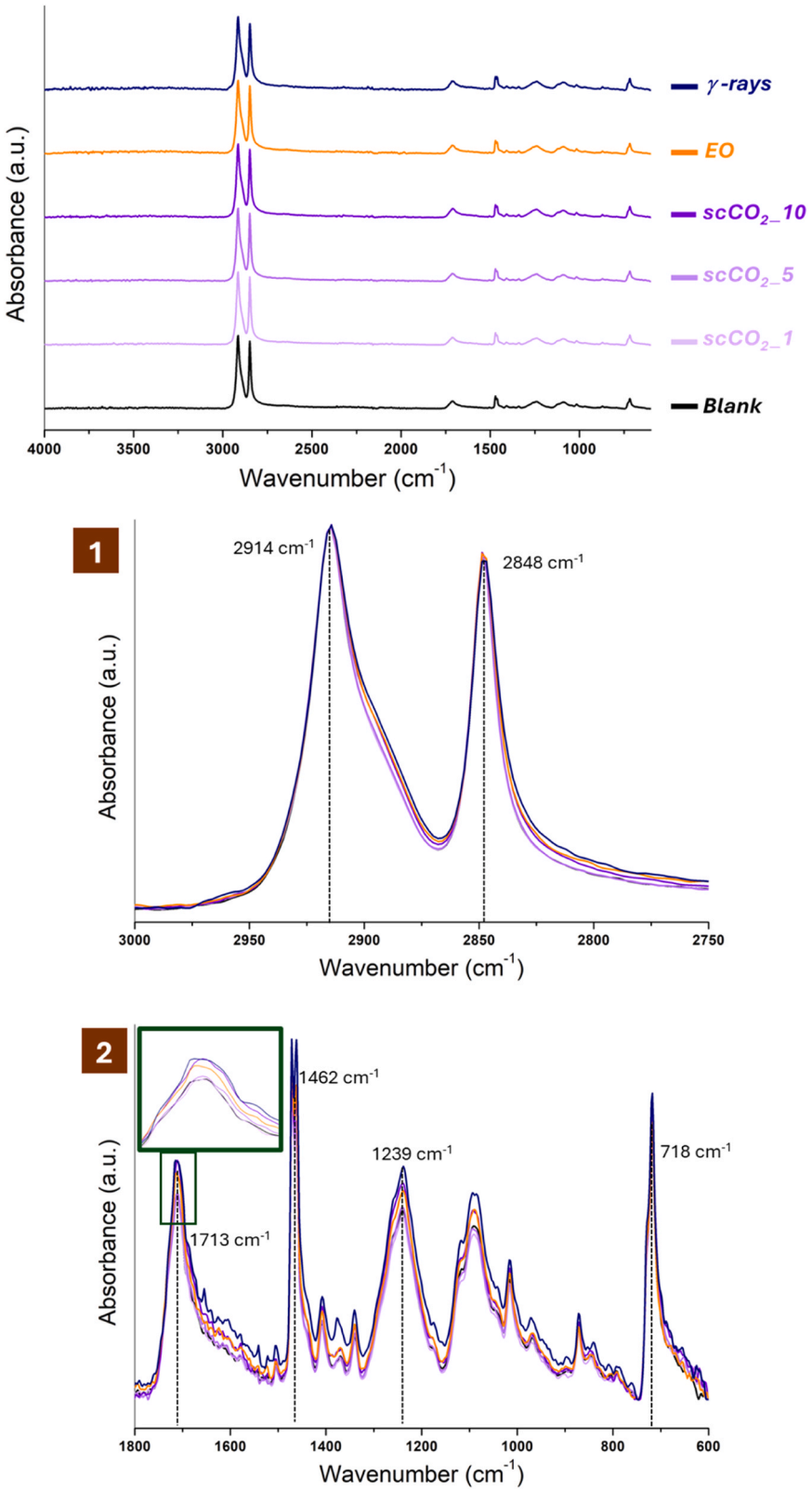

Fig. 5. FTIR spectra of PE spunbond filter of *EF facemasks*. Enlarged regions: (1) Between 2750 and 3000 cm^{-1} and (2) between 600 and 1800 cm^{-1}.

Fig. 6.1), there are several bands corresponding to the symmetric and asymmetric stretching vibrations of the -CH_3 and -CH_2 groups [74,75]. Specifically, the band at 2875 cm^{-1} was associated with symmetrical stretching vibration of -CH_3 group. The most obvious change in this magnification compared to the blank is the greater intensity presented by the sample treated with γ-rays. Two characteristic bands at 1455 and 1375 cm^{-1} can be identified in the region between 1300 and 1800 cm^{-1} (region 2 in Fig. 6.2), related to the asymmetric and symmetric bending vibrations of the -CH_2 group [74]. In this instance, both *EO* and *γ-rays* samples also exhibited peaks of higher intensity. Despite the absence of a

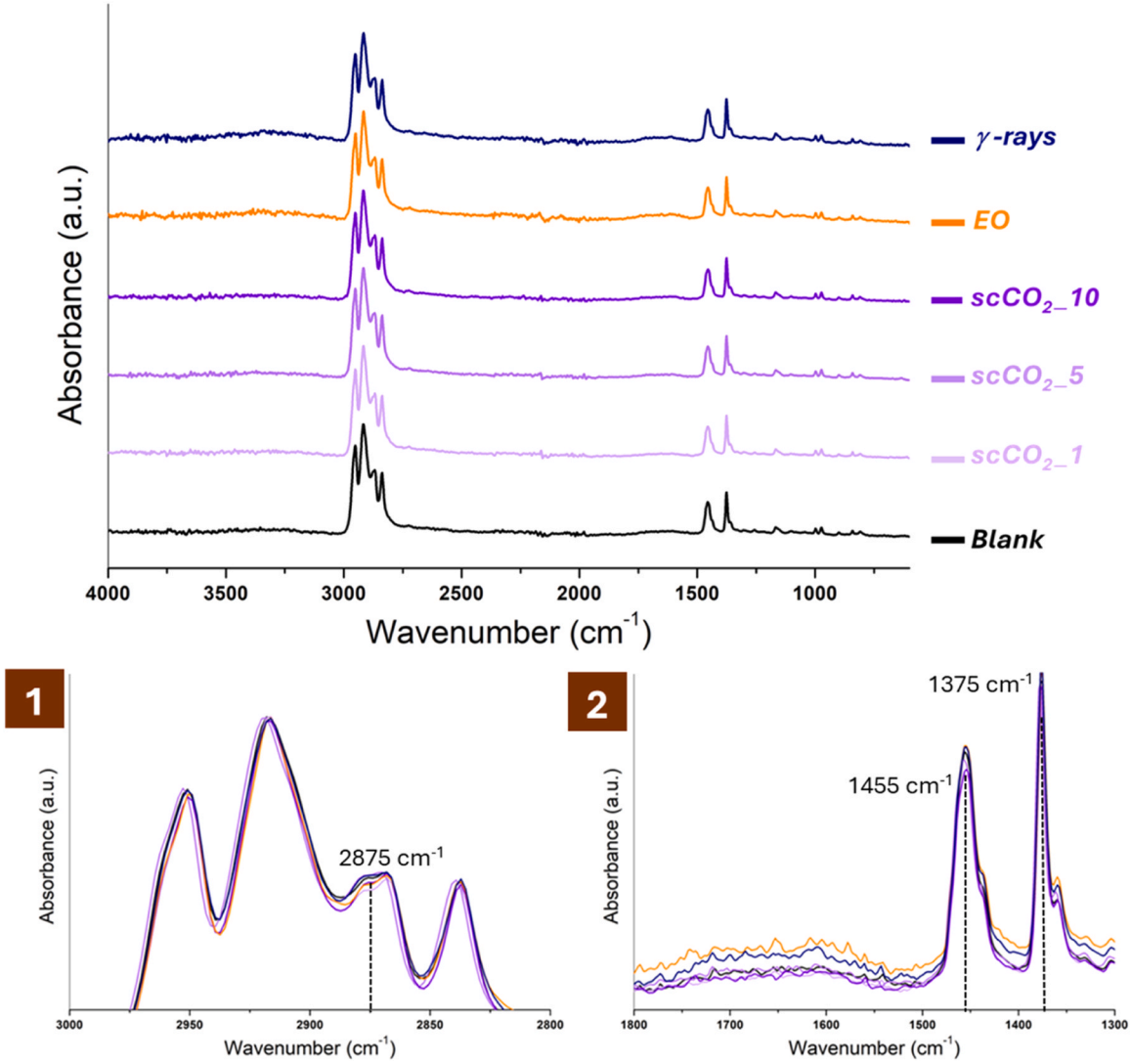

Fig. 6. FTIR spectra of PP meltblown filter of *EF facemask*. Enlarged regions: (1) Between 2800 and 3000 cm^{-1}, and (2) between 1300 and 1800 cm^{-1}.

clearly defined band at 1700 cm^{-1}, a wide band was detected at this region in those facemasks treated with EO and γ-rays and associated with the presence of C═O groups. Previous studies related the presence of this band to the oxidation of PP-based materials after subjecting to different γ-radiation doses [76].

Fig. 7 shows the infrared spectra of *MF facemask* filter composed of PVDF. In Fig. 7.1, in which the range 2750–3500 cm^{-1} is enlarged, the bands 2918 and 2850 cm^{-1} were assigned to the stretching vibration of the group CH_2 and to the symmetrical and asymmetrical vibration of CF_2 [77,78]. These bands, as well as others in the 2800–3100 cm^{-1} range, increased their intensity after the treatment with γ-rays and decreased it after the different cycles of $scCO_2$. The set of wide bands between 1500 and 1700 cm^{-1}, and the band at 799 cm^{-1}, related to double bonds C═C, were the most affected after the treatment with γ-rays. The band at 1147 cm^{-1} (enlarged in Fig. 7.2) was assigned to the symmetrical stretching of the group CF_2, whereas the band located at *ca.* 1069 cm^{-1} was assigned to the waging of C-F bond. The three bands at 761, 839 and 875 cm^{-1} corresponded to the deformation vibration and stress bond vibration of the bond CF_2, to the rocking vibration of the group CH_2 and to the asymmetrical stretching vibration of the group CF_2, respectively. The chemical changes experienced on the polymer were related to its oxidation and degradation, which were previously reported for the treatments with γ-rays [79]. The alterations caused by $scCO_2$ can be attributed to the fact that fluorinated polymers, such as PVDF, can absorb CO_2 molecules, which firstly occupy empty spaces and then move into the amorphous regions [80,81].

4. Conclusions

A sterilization treatment based on $scCO_2$ is herein proposed for FFP2 facemasks as a viable alternative to conventional techniques currently on the market. The versatility of the method demonstrates to be suitable for two types of facemasks: electrostatic (*EF*) and mechanical (*MF*) filter-based masks. $ScCO_2$ treatment induced new electrostatic charges on the facemask filters. These modifications proved particularly beneficial for *MF facemasks*, which continued to meet ISO requirements, as the CO_2 treatment imparted electrostatic charges to the material that were absent in the untreated samples. No significant changes were observed in the mechanical behavior of the elastic bands compared to the untreated samples. The $scCO_2$ treatment induced a relaxation effect in the fibers preserving their structural integrity, whereas the EO and γ-ray techniques resulted in crack formation and breakage in the filter fibers of the facemasks. No chemical changes were obtained in the filters of the masks even after 10 cycles of $scCO_2$ sterilization, in contrast to the chemical alterations detected when treated with γ-rays. Results obtained under controlled laboratory conditions highlight the potential of $scCO_2$ as a sterilization method that preserves the structural and functional integrity of materials, offering an environmentally friendly sterilization

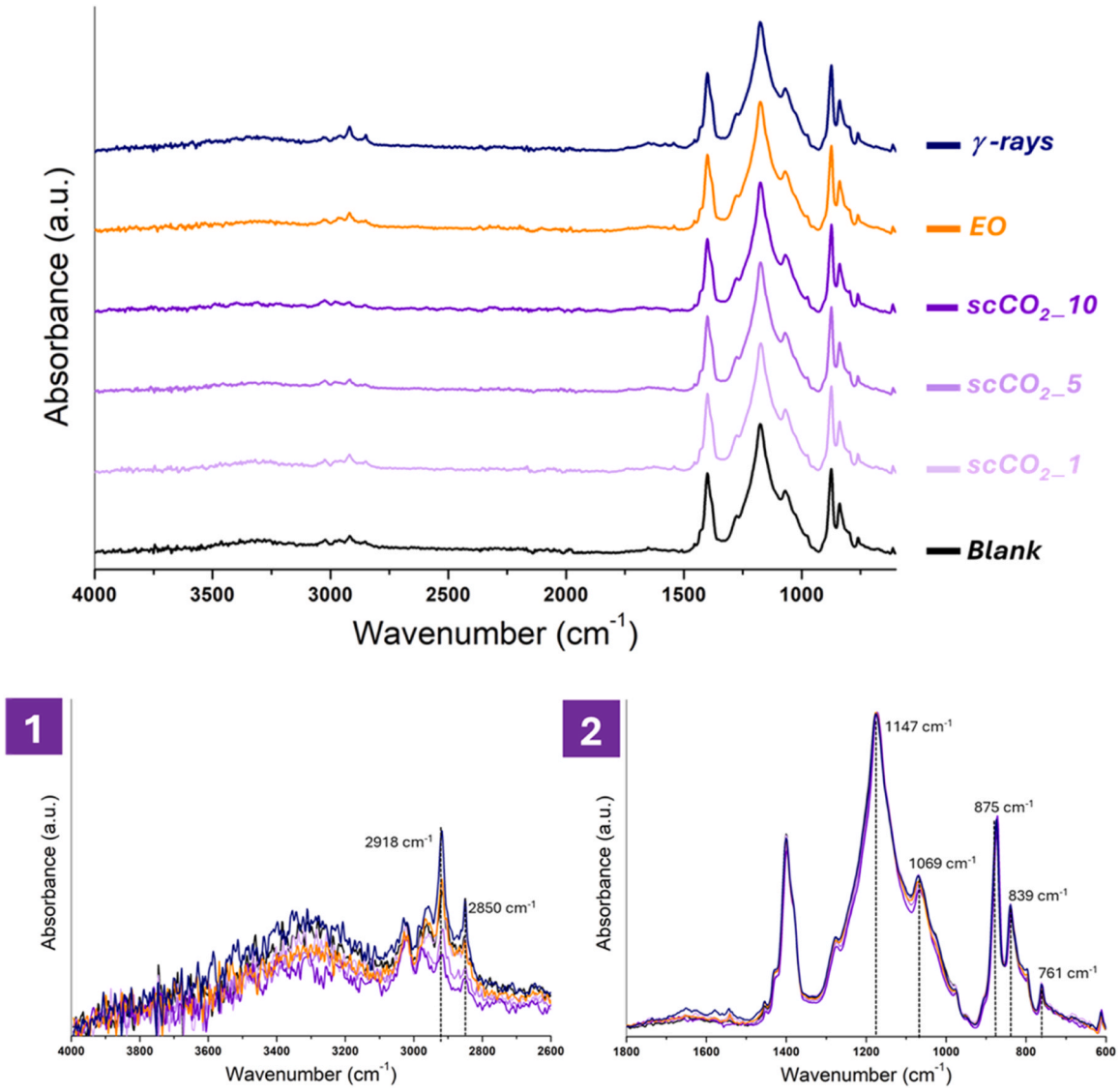

Fig. 7. Spectra of electrospun PVDF nanofiber-based filter of *MF facemasks*. (1) Enlarged region between 2600 and 4000 cm^{-1} and (2) Enlarged region between 600 and 1800 cm^{-1}.

alternative that valorizes and reuses CO_2. Further studies will include the testing of the effect of breathing humidity or repeated donning to confirm the strong potential of this method for safe and effective mask reuse.

CRediT authorship contribution statement

María Carracedo-Pérez: Writing – review & editing, Writing – original draft, Methodology, Investigation. **Cristina Prieto:** Writing – review & editing, Writing – original draft, Methodology, Investigation, Funding acquisition. **María Blanco-Vales:** Writing – review & editing, Writing – original draft, Methodology. **Beatriz Magariños:** Writing – review & editing, Supervision, Methodology, Investigation, Funding acquisition, Conceptualization. **Clara López-Iglesias:** Writing – review & editing, Writing – original draft, Supervision, Methodology, Investigation, Funding acquisition. **Carlos A. García-González:** Writing – review & editing, Writing – original draft, Supervision, Methodology, Investigation, Funding acquisition, Conceptualization.

Declaration of Competing Interest

All authors declare no financial or personal relationships that may be perceived as influencing their work.

Acknowledgements

This work was funded by MICIU/AEI/10.13039/501100011033 [grants PID2023–151340OB-I00 and PDC2022–133526-I00], Xunta de Galicia [ED431C2022/2023], ERDF/EU and European Union NextGenerationEU/PRTR. C.L.-I. acknowledges Xunta de Galicia for a postdoctoral fellowship [ED481B-2021–008]. Work carried out in the framework of the ECO-AERoGELS COST Innovators' Grant (ref. IG18125) and funded by the European Commission. C.P. acknowledges the funding received from the European EU4Health program (2G-Proveil - 101203379) and from CSIC through the Grants to tenured scientists from OEP 2020–2021 (2024ICT225), and the accreditation as Center of Excellence Severo Ochoa CEX2021–001189-S funded by MCIU/AEI/10.13039/501100011033. C. Alvarez-Lorenzo is acknowledged for technical support with the mechanical tests.

Appendix A. Supporting information

Supplementary data associated with this article can be found in the online version at doi:10.1016/j.jece.2025.118991.

Data availability

Data will be made available on request.

References

[1] S. Adanur, A. Jayswal, Filtration mechanisms and manufacturing methods of face masks: an overview, J. Ind. Text. 51 (2022) 3683S–3717S.
[2] A.-B. Wang, X. Zhang, L.-J. Gao, T. Zhang, H.-J. Xu, Y.-J. Bi, A review of filtration performance of protective masks, Int. J. Environ. Res. Public Health 20 (2023) 2346.
[3] J.T.J. Ju, L.N. Boisvert, Y.Y. Zuo, Face masks against COVID-19: Standards, efficacy, testing and decontamination methods, Adv. Colloid Interface Sci. 292 (2021) 102435.
[4] Approved Particulate Filtering Facepiece Respirators | NPPTL | NIOSH | CDC, (2022).
[5] S.M. Imani, L. Ladouceur, T. Marshall, R. Maclachlan, L. Soleymani, T.F. Didar, Antimicrobial nanomaterials and coatings: Current mechanisms and future perspectives to control the spread of viruses including SARS-CoV-2, ACS Nano 14 (2020) 12341–12369.
[6] D.A. Montero, C. Arellano, M. Pardo, R. Vera, R. Gálvez, M. Cifuentes, M. A. Berasain, M. Gómez, C. Ramírez, R.M. Vidal, Antimicrobial properties of a novel copper-based composite coating with potential for use in healthcare facilities, Antimicrob. Resist. Infect. Control 8 (2019) 3.
[7] A. Sahu, K. Mallick, A.P. Das, Environmental impact of Single-Use synthetic face mask and its recycling: a sustainable approach, in: A.P. Das, S. Mishra (Eds.), Impact of COVID-19 Waste on Environmental Pollution and Its Sustainable Management, Springer Nature Switzerland, Cham, 2024, pp. 197–212.
[8] G. Song, H. Cao, L. Liu, M. Jin, Analysis of marine microplastic pollution of disposable masks under COVID-19 Epidemic—A DPSIR framework, IJERPH 19 (2022) 16299.
[9] M. Mohanty, J. Mohanty, S. Dey, K. Dutta, M.P. Shah, A.P. Das, The face mask: A tale from protection to pollution and demanding sustainable solution, Emerg. Contam. 10 (2024) 100298.
[10] E. Lemiech-Mirowska, Z. Kiersnowska, M. Michałkiewicz, A. Depta, M. Marczak, Nosocomial infections as one of the most important problems of healthcare system, Ann. Agric. Environ. Med 28 (2021) 361–366.
[11] M. Traverse, H. Aceto, Environmental cleaning and disinfection, Vet. Clin. North Amer. Small Anim. Pract. 45 (2015) 299–330.
[12] M. Jayabalan, Sterilization and reprocessing of materials and medical Devices—Reusability, J. Biomater. Appl. 10 (1995) 97–112.
[13] ANSI/AAMI ST67:2011 (ANSI/AAMI ST 67:2011) - Sterilization of health care products - Requirements and guidance for selecting a sterility assurance level (SAL) for products labeled “sterile,”.
[14] M. Tao, T. Ao, X. Mao, X. Yan, R. Javed, W. Hou, Y. Wang, C. Sun, S. Lin, T. Yu, Q. Ao, Sterilization and disinfection methods for decellularized matrix materials: Review, consideration and proposal, Bioact. Mater. 6 (2021) 2927–2945.
[15] A. Kumar, S.B. Kasloff, A. Leung, T. Cutts, J.E. Strong, K. Hills, G. Vazquez-Grande, B. Rush, S. Lother, R. Zarychanski, J. Krishnan, N95 Mask Decontamination using Standard Hospital Sterilization Technologies, PLoS ONE 15 (12) (2020).
[16] AENOR, ISO 17665-1:2006 Sterilization of health care products-Moist heat-Part 1: Requirements for the development, validation and routine control of a sterilization process for medical devices.
[17] W.J. Rogers, Chapter 2: steam and dry heat sterilization of biomaterials and medical devices, in: Sterilisation of Biomaterials and Medical Devices, Elsevier, 2012, pp. 20–55.
[18] J.Y. Teo, J. Kng, B. Periaswamy, S. Liu, P.-C. Lim, C.E. Lee, B.H. Tan, X.J. Loh, X. Ni, D. Tiang, G. Yi, Y.Y. Ong, M.L. Ling, W.Y. Wan, H.M. Wong, M. How, X. Xin, Y. Zhang, Y.Y. Yang, Exploring reusability of disposable face masks: Effects of disinfection methods on filtration efficiency, breathability, and fluid resistance, Glob. Chall. 5 (2021) 2100030.
[19] K.E. Zulauf, A.B. Green, A.N. Nguyen Ba, T. Jagdish, D. Reif, R. Seeley, A. Dale, J. E. Kirby, Microwave-Generated steam decontamination of N95 respirators utilizing universally accessible materials, mBio 11 (2020), https://doi.org/10.1128/mbio.00997-20.
[20] AENOR, ISO 11135:2014 Sterilization of health care products-Ethylene oxide-Part 1:Requirements for the development, validation and routine control of a sterilization process for medical devices.
[21] Q.-Q. Qiu, W.-Q. Sun, J. Connor, Sterilization of biomaterials of synthetic and biological origin, in: Comprehensive Biomaterials, Elsevier, 2011, pp. 127–144.
[22] M. Zimniewska, H. Witmanowski, A. Kicinska-Jakubowska, A. Jundzill, E. Kwiatkowska, B. Romanowska, L.B. Malinowski, Assessment of the possibility of surgical masks re-use after a sterilization process in the pandemic condition of COVID-19, Text. Res. J. 92 (2022) 3082–3096.
[23] W.A. Rutala, D.J. Weber, Sterilization of 20 billion medical devices by ethylene oxide (ETO): Consequences of ETO closures and alternative sterilization technologies/solutions, Amer. J. Infect. Control 51 (2023) A82–A95.
[24] K. Steenland, L. Stayner, A. Greife, W. Halperin, R. Hayes, R. Hornung, S. Nowlin, Mortality among workers exposed to ethylene oxide, New Engl. J. Med. 324 (1991) 1402–1407.
[25] A. Sobaszek, J.C. Hache, P. Frimat, V. Akakpo, G. Victoire, D. Furon, Working conditions and health effects of ethylene oxide exposure at hospital sterilization sites, J. Occup. Environ. Med. 41 (1999) 492.
[26] C. Kirman, A. Li, P. Sheehan, J. Bus, R. Lewis, S. Hays, Ethylene oxide review: Characterization of total exposure via endogenous and exogenous pathways and their implications to risk assessment and risk management, J. Toxicol. Environ. Health Part B 24 (2021) 1–29.
[27] AENOR, ISO 11137-1:2006 Sterilization of health care products-Radiation-Part 1: Requirements for development, validation and routine control of a sterilization process for medical devices.
[28] N.P. Tipnis, D.J. Burgess, Sterilization of implantable polymer-based medical devices: A review, Int. J. Pharm. 544 (2018) 455–460.
[29] C.K. Herczeg, J. Song, Sterilization of polymeric implants: Challenges and opportunities, ACS Appl. Bio Mater. 5 (2022) 5077–5088.
[30] L. Cortella, C. Albino, K. Froment, P. Cinquin, J.-P. Alcaraz, S. Rouif, L. Coq, A. Joubert, Y. Andres, Feasibility of gamma or e-beam irradiation as a treatment for reuse of medical masks after a first use, Int. At. Energy Agency (IAEA) (2020).
[31] I. Gouzman, H. Datz, R. Verker, A. Bolker, L. Epstein, L. Buchbinder, Y. Freid, E. Sarid, E. Zuckerman, G. Boaz, The feasibility of sterilization for reuse of disposable medical equipment: Gamma irradiation of medical masks and medical protective clothing, Int. At. Energy Agency (IAEA) (2020).
[32] N. Ribeiro, G.C. Soares, V. Santos-Rosales, A. Concheiro, C. Alvarez-Lorenzo, C. A. García-González, A.L. Oliveira, A new era for sterilization based on supercritical CO_2 technology, J. Biomed. Mater. Res. 108 (2020) 399–428.
[33] S. Basak, R.S. Singhal, The potential of supercritical drying as a “Green” method for the production of food-grade bioaerogels: A comprehensive critical review, Food Hydrocoll. 141 (2023) 108738.
[34] M. Carracedo-Pérez, I. Ardao, C. López-Iglesias, B. Magariños, C.A. García-González, Direct and green production of sterile aerogels using supercritical fluid technology for biomedical applications, J. CO2 Util. 86 (2024) 102891.
[35] H.K. Ruiz, M. Ruiz, A. Cabañas, L. Calvo, Inactivation of *Staphylococcus epidermidis* in a cotton gauze with supercritical CO_2 modified with essential oils, Processes 12 (2024) 2158.
[36] A. Tabernero, Á. González-Garcinuño, S. Cardea, E. Martín Del Valle, Supercritical carbon dioxide and biomedicine: Opening the doors towards biocompatibility, Chem. Eng. J. 444 (2022) 136615.
[37] D. Bennet, A.F. Harris, J. Lacombe, C. Brooks, N. Bionda, A.D. Strickland, T. Eisenhut, F. Zenhausern, Evaluation of supercritical CO_2 sterilization efficacy for sanitizing personal protective equipment from the coronavirus SARS-CoV-2, Sci. Total Environ. 780 (2021) 146519.
[38] L. Andrée, J. Dodemont, H.R. Harhangi, K. Dijkstra, L. van Niftrik, F. Yang, S.C. G. Leeuwenburgh, Inactivation of *Staphylococcus aureus* in gelatin nanoparticles using supercritical carbon dioxide, J. Supercrit. Fluids (2023) 105979.
[39] C.S.A. Bento, S. Alarico, N. Empadinhas, H.C. de Sousa, M.E.M. Braga, Sequential $scCO_2$ drying and sterilisation of alginate-gelatine aerogels for biomedical applications, J. Supercrit. Fluids 184 (2022) 105570.
[40] F. Zani, C. Veneziani, E. Bazzoni, L. Maggi, G. Caponetti, R. Bettini, Sterilization of corticosteroids for ocular and pulmonary delivery with supercritical carbon dioxide, Int. J. Pharm. 450 (2013) 218–224.
[41] J.D. Hemmer, M.J. Drews, M. LaBerge, M.A. Matthews, Sterilization of bacterial spores by using supercritical carbon dioxide and hydrogen peroxide, J. Biomed. Mater. Res. B. 80B (2007) 511–518.
[42] J. Zhang, S. Burrows, C. Gleason, M.A. Matthews, M.J. Drews, M. LaBerge, Y.H. An, Sterilizing *Bacillus pumilus* spores using supercritical carbon dioxide, J. Microbiol. Methods 66 (2006) 479–485.
[43] AENOR, UNE-EN ISO 11140-1:2015 Esterilización de productos para atención sanitaria Indicadores químicos Parte 1: Requisitos generales (ISO 11140-1:2014).
[44] V. Santos-Rosales, B. Magariños, R. Starbird, J. Suárez-González, J.B. Fariña, C. Alvarez-Lorenzo, C.A. García-González, Supercritical CO_2 technology for one-pot foaming and sterilization of polymeric scaffolds for bone regeneration, Int. J. Pharm. 605 (2021) 120801.
[45] M. Zourob, S. Elwary, A. Turner, Principles of bacterial detection: biosensors, recognition receptors and microsystems, Springer, New York, NY, 2008.
[46] V. Santos-Rosales, C. López-Iglesias, A. Sampedro-Viana, C. Alvarez-Lorenzo, S. Ghazanfari, B. Magariños, C.A. García-González, Supercritical CO_2 sterilization: an effective treatment to reprocess FFP3 face masks and to reduce waste during COVID-19 pandemic, Sci. Total Environ. 826 (2022) 154089.
[47] +A1 Respiratory protective devices Filtering half masks to protect against particles Requirements, testing, marking, Asociación Española de Normalización, UNE-EN 149.
[48] ASTM D5034 Standard Test Method for Breaking Strength and Elongation of Textile Fabrics (Grab Test).
[49] V. Warambourg, A. Mouahid, C. Crampon, A. Galinier, M. Claeys-Bruno, E. Badens, Supercritical CO_2 sterilization under low temperature and pressure conditions, J. Supercrit. Fluids 203 (2023) 106084.
[50] Q.-Q. Qiu, P. Leamy, J. Brittingham, J. Pomerleau, N. Kabaria, J. Connor, Inactivation of bacterial spores and viruses in biological material using supercritical carbon dioxide with sterilant, J. Biomed. Mater. Res. B. 91B (2009) 572–578.
[51] D.M. Bednarski, E.E. Lantz, C.E. Bobst, A.R. Eisenhut, S.J. Eyles, J.P. Fey, Sterilization of epidermal growth factor with supercritical carbon dioxide and peracetic acid; analysis of changes at the amino acid and protein level, Biochim. Et. Biophys. Acta (BBA) Proteins Proteom. 1868 (2020) 140334.

[52] A. Bernhardt, M. Wehrl, B. Paul, T. Hochmuth, M. Schumacher, K. Schütz, M. Gelinsky, Improved sterilization of sensitive biomaterials with supercritical carbon dioxide at low temperature, PLoS ONE 10 (2015) e0129205.
[53] C. Blazejewski, F. Wallet, A. Rouzé, R. Le Guern, S. Ponthieux, J. Salleron, S. Nseir, Efficiency of hydrogen peroxide in improving disinfection of ICU rooms, Crit. Care 19 (2015) 30.
[54] P.A. Indelicato, 28 - chemical sterilization techniques for allograft preparation for anterior cruciate ligament reconstruction, in: C.C. Prodromos (Ed.), The Anterior Cruciate Ligament, 2nd ed., Elsevier, 2018, pp. 117–120. .e1.
[55] R.R. Mallepally, M.A. Marin, N. Montesdeoca, C. Parrish, K.R. Ward, M.A. McHugh, Hydrogen peroxide loaded cellulose acetate mats as controlled topical O_2 delivery devices, J. Supercrit. Fluids 105 (2015) 77–83.
[56] M. Yousefimashouf, R. Yousefimashouf, M.S. Alikhani, H. Hashemi, P. Karami, Z. Rahimi, S.M. Hosseini, Evaluation of the bacterial contamination of face masks worn by personnel in a center of COVID 19 hospitalized patients: a cross-sectional study, N. Microbes N. Infect. 52 (2023) 101090.
[57] H.K. Ruiz, A. Cabañas, L. Calvo, Sterilisation and virus SARS-CoV-2 inactivation in personal protective equipment with supercritical CO_2, J. Ind. Eng. Chem. (2025).
[58] R. Zulli, C. Del Vecchio, P. Andrigo, V. Conciatori, F. Santi, A. Zambon, E. Lavezzo, S. Spilimbergo, SARS-CoV-2 inactivation by supercritical carbon dioxide coupled with hydrogen peroxide, J. Supercrit. Fluids 210 (2024) 106272.
[59] R. Jeong, H. Kumar, S. Jones, A. Sandwell, K. Kim, S.S. Park, Increased sanitization potency of hydrogen peroxide with synergistic O_3 and intense pulsed light for non-woven polypropylene, RSC Adv. 11 (2021) 23881–23891.
[60] M. Carsí, M. Alonso, Influence of aerosol electrical charging state and time of use on the filtration performance of some commercial face masks for 10–150 nm particles, J. Aerosol Sci. 159 (2022) 105849.
[61] V. Puderbach, R. Kirsch, S. Antonyuk, Experimental characterization of the mechanical properties of filter media in Solid–Liquid filtration processes, Materials 17 (2024) 4578.
[62] M. Tohfafarosh, D. Baykal, J.W. Kiel, K. Mansmann, S.M. Kurtz, Effects of gamma and e-beam sterilization on the chemical, mechanical and tribological properties of a novel hydrogel, J. Mech. Behav. Biomed. Mater. 53 (2016) 250–256.
[63] M.H. Shojaie, A.H. Hemmasi, M. Talaeipour, E. Ghasemi, Effect of gamma-ray and melt flow index of polypropylene on the properties of the lignocellulosic composite, Radiat. Phys. Chem. 177 (2020) 109126.
[64] R. Halamicek, C. Wiesmann, R. Kröner, M. Eber, C. Bogdan, D.W. Schubert, Influence of different treatment conditions on the filtration performance of conventional electret melt blown non-woven and novel nano FFP2 masks, PLoS One 18 (2023) e0291679.
[65] Z. Peng, J. Shi, X. Xiao, Y. Hong, X. Li, W. Zhang, Y. Cheng, Z. Wang, W.J. Li, J. Chen, M.K.H. Leung, Z. Yang, Self-charging electrostatic face masks leveraging triboelectrification for prolonged air filtration, Nat. Commun. 13 (2022) 7835.
[66] M. Champeau, J.-M. Thomassin, C. Jérôme, T. Tassaing, In situ FTIR micro-spectroscopy to investigate polymeric fibers under supercritical carbon dioxide: CO_2 sorption and swelling measurements, J. Supercrit. Fluids 90 (2014) 44–52.
[67] Z. Jia, C. Duan, Preparation and characterization of surface modified PPTA fibers by Ultrasonic-Assisted hydrogen peroxide solutions, Fibers Polym. 20 (2019) 2310–2316.
[68] C. Maier, T. Calafut, Polypropylene: the Definitive User's Guide and Databook, Plastics Design Library, Norwich, NY, 1998.
[69] B. Bonavoglia, G. Storti, M. Morbidelli, A. Rajendran, M. Mazzotti, Sorption and swelling of semicrystalline polymers in supercritical CO_2, J. Polym. Sci. Part B Polym. Phy. 44 (2006) 1531–1546.
[70] J.V. Gulmine, P.R. Janissek, H.M. Heise, L. Akcelrud, Polyethylene characterization by FTIR, Polym. Test. 21 (2002) 557–563.
[71] B. Smith, The infrared spectra of polymers II, Polyethylene 36 (2021) 24–29.
[72] D. Amelia, E. Fathul Karamah, M. Mahardika, E. Syafri, S. Mavinkere Rangappa, S. Siengchin, M. Asrofi, Effect of advanced oxidation process for chemical structure changes of polyethylene microplastics, Mater. Today. Proc. 52 (2022) 2501–2504.
[73] J.L. Ellis, J.C. Titone, D.L. Tomasko, N. Annabi, F. Dehghani, Supercritical CO_2 sterilization of ultra-high molecular weight polyethylene, J. Supercrit. Fluids 52 (2010) 235–240.
[74] N. Chibani, H. Djidjelli, A. Dufresne, A. Boukerrou, S. Nedjma, Study of effect of old corrugated cardboard in properties of polypropylene composites: study of mechanical properties, thermal behavior, and morphological properties, J. Vinyl Addit. Technol. 22 (2016) 231–238.
[75] B. Smith, The Infrared Spectra of Polymers III: Hydrocarbon Polymers, Spectroscopy 36 (2021) 22–25.
[76] S. Mouaci, M. Saidi, N. Saidi-Amroun, Oxidative degradation and morphological properties of gamma-irradiated isotactic polypropylene films, Micro Nano Lett. 12 (2017) 478–481.
[77] H. Yuan, J. Ren, Preparation of poly(vinylidene fluoride) (PVDF)/acetalyzed poly (vinyl alcohol) ultrafiltration membrane with the enhanced hydrophilicity and the anti-fouling property, Chem. Eng. Res. Des. 121 (2017) 348–359.
[78] T.T.V. Tran, S.R. Kumar, S.J. Lue, Separation mechanisms of binary dye mixtures using a PVDF ultrafiltration membrane: Donnan effect and intermolecular interaction, J. Membr. Sci. 575 (2019) 38–49.
[79] Y. Guo, C. Liu, H. Liu, W. Wang, H. Li, C. Zhang, Influences of gamma-ray irradiation on PVDF membrane behavior: An experimental study based on simulation and numerical analysis, Polym. Degrad. Stab. 193 (2021) 109722.
[80] A. Zeinolebadi, J. Schwaderer, S. Beuermann, T. von Ostrowski, P. Jaeger, Effects of supercritical carbon dioxide sorption on the microstructure of poly(vinylidene fluoride), J. Supercrit. Fluids 177 (2021) 105347.
[81] J. Li, Q. Meng, W. Li, Z. Zhang, Influence of crystalline properties on the dielectric and energy storage properties of poly(vinylidene fluoride), J. Appl. Polym. Sci. 122 (2011) 1659–1668.